Acta Crystallographica Section F
Structural Biology and Crystallization Communications
ISSN 1744-3091

Crystallization and preliminary X-ray diffraction studies of the terminal oxygenase component of carbazole 1,9a-dioxygenase from *Nocardioides aromaticivorans* IC177

Kengo Inoue,[a] Yuji Ashikawa,[a] Yusuke Usami,[a] Haruko Noguchi,[a,b] Zui Fujimoto,[c] Hisakazu Yamane[a] and Hideaki Nojiri[a,b]*

[a]Biotechnology Research Center, The University of Tokyo, 1-1-1 Yayoi, Bunkyo-ku, Tokyo 113-8657, Japan, [b]Professional Programme for Agricultural Bioinformatics, The University of Tokyo, 1-1-1 Yayoi, Bunkyo-ku, Tokyo 113-8657, Japan, and [c]Department of Biochemistry, National Institute of Agrobiological Sciences, 2-1-2 Kannondai, Tsukuba, Ibaraki 305-8602, Japan

Correspondence e-mail: anojiri@mail.ecc.u-tokyo.ac.jp

Received 14 September 2006
Accepted 27 October 2006

Carbazole 1,9a-dioxygenase (CARDO) catalyzes the dihydroxylation of carbazole by angular-position (C9a) carbon bonding to the imino nitrogen and its adjacent C1 carbon. CARDO consists of a terminal oxygenase component and two electron-transfer components: ferredoxin and ferredoxin reductase. The terminal oxygenase component (43.9 kDa) of carbazole 1,9a-dioxygenase from *Nocardioides aromaticivorans* IC177 was crystallized at 293 K using the hanging-drop vapour-diffusion method with PEG 8000 as the precipitant. The crystals diffract to 2.3 Å resolution and belong to space group *C*2.

1. Introduction

Rieske nonhaem iron oxygenase systems (ROSs) are the initial catalysts in the degradation pathways of various environmentally important aromatic compounds, including dioxins, polychlorinated biphenyls and crude-oil components such as polycyclic aromatic hydrocarbons and carbazole (Wittich, 1998; Bressler & Fedorak, 2000; Nojiri & Omori, 2002; Habe & Omori, 2003; Furukawa *et al.*, 2004). The ROSs catalyze a dihydroxylation reaction, in the initial step of which the C atoms bonded to the carbazole N atom and the adjacent C atom from the aromatic ring are hydroxylated (Fig. 1). This reaction, called angular dioxygenation, is catalyzed by a limited number of ROSs, which are called angular dioxygenases (Nojiri & Omori, 2002). These enzymes typically consist of two or three components that comprise an electron-transfer chain that mobilizes electrons from NADH or NADPH *via* flavin and the [2Fe–2S] redox centres of the dioxygen activation site.

The ROSs have been classified into five groups, IA, IB, IIA, IIB and III, based on their number of constituents and the nature of their redox centres (Batie *et al.*, 1991).

The Gram-positive carbazole degrader *Nocardioides aromaticivorans* IC177 possesses *carAaAcAd* genes encoding the angular dioxygenase system carbazole 1,9a-dioxygenase (CARDO; Fig. 1; Inoue *et al.*, 2005, 2006). CARDO consists of three components: the terminal oxygenase CARDO-O, the ferredoxin CARDO-F and the ferredoxin reductase CARDO-R, which are encoded by the *carAa*, *carAc* and *carAd* genes, respectively. The CARDO of *N. aromaticivorans* IC177 is classified into the class IIB ROSs (Inoue *et al.*, 2006), while the well studied CARDOs from *Pseudomonas resinovorans* CA10 and *Sphingomonas* sp. KA1 are classified into classes III and IIA, respectively (Sato *et al.*, 1997; Inoue *et al.*, 2004; Urata *et al.*, 2006). CARDOs possess diverse types of electron-transfer components (*e.g.* CARDO-F and CARDO-R) and have a high similarity (>45% identity at the amino-acid sequence level) within the terminal oxygenase. Although the structures of several ROSs proteins are known (Ferraro *et al.*, 2005), it is not clear how the electron donors interact with the recipient molecules and the precise nature of the electron-transfer mechanism remains to be determined. Therefore, CARDO is an excellent model system for studying the structure–function relationships of ROS-like enzymes and the mechanism of electron transfer. The structures of the terminal oxygenase components of ROSs determined to date have all demonstrated an α_3 or $\alpha_3\beta_3$ configuration with threefold symmetry (Ferraro *et al.*, 2005). Recently, we determined the crystal structures

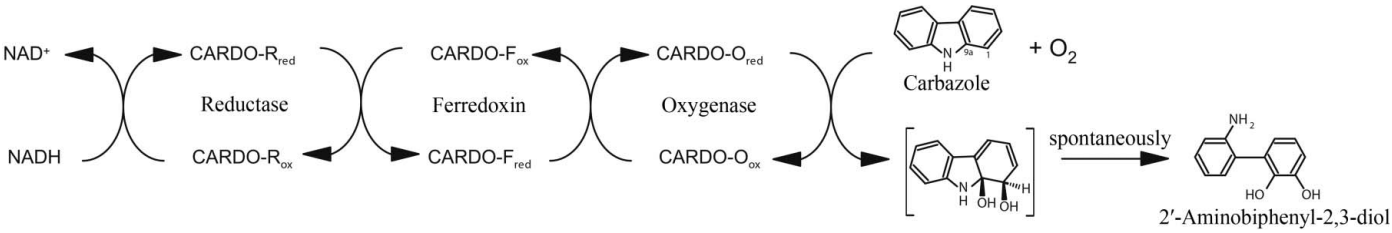

Figure 1
Components and functions of the CARDO system. The proposed electron-transfer reactions and the conversion of carbazole to 2′-aminobiphenyl-2,3-diol are illustrated. The subscripts 'ox' and 'red' indicate the oxidized and reduced states of the CARDO components, respectively.

of CARDO-O from *Janthinobacterium* sp. J3 (99% amino-acid sequence identity to that of *P. resinovorans* CA10; Inoue *et al.*, 2004; Nojiri *et al.*, 2005) and CARDO-O from *Sphingomonas* sp. KA1 (Katsuki *et al.*, unpublished data), which revealed both CARDO-Os to have α_3 subunit configuration. We also determined the structures of CARDO-F from *P. resinovorans* CA10 (Nam *et al.*, 2005) and the complex of CARDO-O of *Janthinobacterium* sp. J3 with CARDO-F of *P. resinovorans* CA10 (Ashikawa *et al.*, 2005). Based on the structure of the complex of CARDO-O of *Janthinobacterium* sp. J3 with CARDO-F of *P. resinovorans* CA10, we proposed the interacting sites in the respective components (Ashikawa *et al.*, 2006). Therefore, comparison of the molecular surface of CARDO-O of *Janthinobacterium* sp. J3 and that of *N. aromaticivorans* IC177 will provide detailed information about the protein–protein interaction that is necessary for electron transfer in this system.

We analyzed the substrate specificities of CARDO from *P. resinovorans* CA10 and *Sphingomonas* sp. KA1 (Nojiri *et al.*, 1999; Habe *et al.*, 2001; Takagi *et al.*, 2002; Urata *et al.*, 2006) and showed that CARDO can catalyze diverse oxygenations with a broad substrate range. Both CARDOs catalyzed the angular dioxygenation of carbazole, dibenzofuran and dibenzo-*p*-dioxin, the monooxygenation of fluorene and the lateral dioxygenation of biphenyl and naphthalene. Previously, we demonstrated that the CARDO of *N. aromaticivorans* IC177 has a different substrate preference from the CARDOs of *P. resinovorans* CA10 and *Sphingomonas* sp. KA1, exhibiting significant activity for carbazole, dibenzo-*p*-dioxin and naphthalene, but far less activity for dibenzofuran and biphenyl (dibenzofuran and biphenyl are preferred substrates for the CARDOs of *P. resinovorans* CA10 and *Sphingomonas* sp. KA1; Inoue *et al.*, 2006).

In this study, we report crystallization and preliminary X-ray diffraction studies on the CARDO-O of *N. aromaticivorans* IC177 (composed of 388 amino acids with a molecular weight of 43.9 kDa).

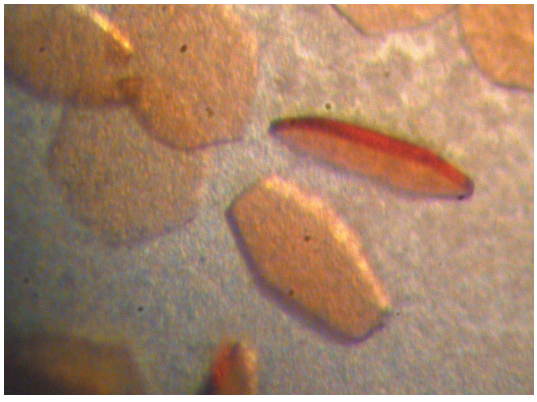

Figure 2
Crystals of CARDO-O from *N. aromaticivorans* IC177.

2. Protein expression and purification

The *carAa* gene (accession No. BAE79498) was PCR-amplified from plasmid pB177103 (Inoue *et al.*, 2006) using primers 5′-TCTAGAGTAAGGAGGTGTTCATATGAGCACCTCTCAGGAAAT-3′ and 5′-ACTAGTAAGCTTTCAGTGGTGGTGGTGGTGGTGCGACATTTCCACTCGGGC-3′. The PCR product was ligated into the pT7Blue T-vector (Novagen). The nucleotide sequence of the insert was checked with the original sequence. The plasmid was digested with *Nde*I and *Hin*dIII. A 1.2 kbp *Nde*I–*Hin*dIII fragment was inserted into overexpression vector pET-26b(+) (Novagen; designated pE177503). pE177503 contains the genes for the full-length CARDO-O subunit with a 6×His tag that replaced the termination codon (ht-CARDO-O). The transformed *Escherichia coli* BL21 (DE3) (Novagen) cells were grown at 303 K on SB medium (Nam *et al.*, 2002) supplemented with 0.5 m*M* IPTG. After 12 h incubation, the cells were harvested by centrifugation at 5000*g* for 10 min, washed twice with TG buffer (Nam *et al.*, 2002) and resuspended in buffer *A* (20 m*M* Tris–HCl pH 7.5 containing 0.5 *M* NaCl and 10% glycerol). The crude cell extract was prepared by sonication and centrifugation at 25 000*g* for 2 h and was applied onto a HiTrap Chelating HP column (GE Healthcare) equipped with an ÄKTA FPLC instrument (GE Healthcare) according to the manufacturer's recommendations. ht-CARDO-O was eluted with buffer *B* (buffer *A* containing 300 m*M* imidazole). The fractions containing ht-CARDO-O were pooled and concentrated by ultrafiltration using Centriprep YM-10 (Millipore). The resultant preparation was further purified by gel-filtration chromatography using a Superdex 200 prep-grade (GE Healthcare) column and GFC buffer (Nam *et al.*, 2002). During purification using gel-filtration chromatography, the molecular weight of the putative α_3 trimer of ht-CARDO-O was estimated as 124 kDa. As the molecular weight of the monomer corresponded to approximately 45 kDa on SDS–PAGE (data not shown), this suggested that ht-CARDO-O indeed forms an α_3 assembly. Prior to crystallization, the purified ht-CARDO-O was confirmed to retain its angular dioxygenation activity for carbazole when coupled with the electron-transfer proteins CARDO-F and CARDO-R from *N. aromaticivorans* IC177 and NADH (data not shown; Fig. 1). These data indicated that CARDO-O from *N. aromaticivorans* IC177 is active as a trimer similar in nature to that of CARDO from *P. resinovorans* CA10 (Nam *et al.*, 2002). Protein concentrations were estimated using a protein-assay kit (Bio-Rad; Bradford, 1976) with BSA as a standard. For crystallization experiments, a solution of the protein in 5 m*M* Tris–HCl pH 7.5 with CARDO-O concentration in the range 5–30 mg ml^{-1} was used.

3. Crystallization

Crystallization was performed using the hanging-drop vapour-diffusion method at 293 K. Drops containing 2 µl protein solution

Table 1
Crystal parameters and data-collection statistics.

The data were collected on AR-NW12 at the Photon Factory, Tsukuba, Japan. Values in parentheses are for the highest resolution shell.

Wavelength (Å)	1.0
Space group	*C*2
Unit-cell parameters (Å, °)	a = 280.0, b = 161.7, c = 194.7, β = 118.7
Resolution range (Å)	50.0–2.30 (2.38–2.30)
Total No. of reflections	2520002
No. of unique reflections	336389 (33466)
Completeness (%)	100 (100)
Average $I/\sigma(I)$	20.4 (4.9)
$R_{\rm sym}$ (%)	8.4 (30.3)
Multiplicity	7.5 (7.3)

† $R_{\rm sym} = \sum_{\mathbf{h}} \sum_l |I_{\mathbf{h}l} - \langle I_{\mathbf{h}} \rangle| / \sum_{\mathbf{h}} \sum_l \langle I_{\mathbf{h}} \rangle$, where I_l is the lth observation of reflection **h** and $\langle I_{\mathbf{h}} \rangle$ is the weighted average intensity for all observations l of reflection **h**.

and 2 µl mother liquor were equilibrated against 800 µl reservoir solution. The initial crystallization conditions were screened using Crystal Screens I and II, Crystal Screen Cryo and Index (Hampton Research). Several crystals were obtained using Crystal Screen Cryo condition No. 50 [12%(*w*/*v*) PEG 8000, 0.4 *M* lithium sulfate and 20%(*v*/*v*) glycerol] in the reservoir and protein solution at a concentration of 30 mg ml^{-1}. The crystals appeared within 3 d and grew to approximate dimensions of 0.2 × 0.2 × 0.02 mm (Fig. 2). Attempts to optimize this condition by changing the pH, precipitant concentration and temperature did not improve the quality of the crystals.

4. X-ray analysis

The crystals were directly flash-cooled in a nitrogen stream at 100 K. Diffraction experiments were conducted at beamline AR-NW12, Photon Factory, Tsukuba, Japan. Diffraction data were collected using a wavelength of 1.0 Å with a Quantum 210 CCD X-ray detector (ADSC). The diffraction data were collected using a single crystal in 0.5° oscillation steps over a range of 360° with a 5 s exposure per frame. The data sets were integrated and scaled using the *HKL*-2000 program suite (Otwinowski & Minor, 1997). A data set was collected to 2.3 Å resolution. The data-collection and processing statistics are summarized in Table 1. The space group of the crystal was determined to be *C*2, with unit-cell parameters a = 280.00, b = 161.66, c = 194.66 Å, β = 118.65°. Initial analysis of the crystal solvent content using the Matthews coefficient (Matthews, 1968) suggested that the asymmetric unit contains five trimers (57.4% solvent content) or six trimers (48.9% solvent content), with an acceptable packing density $V_{\rm M}$ of 2.88 or 2.40 Å^3 Da^{-1}, respectively. The crystal structure solution was attempted using the molecular-replacement method with the structure of ht-CARDO-O from *Sphingomonas* sp. KA1 (49% amino-acid sequence identity; Katsuki *et al.*, structural data unpublished) as a search model. A full description of the structure determination will be published elsewhere.

Part of this work was supported by a Grant-in-Aid for Scientific Research (17380052 to HN) from the Ministry of Education, Culture, Sports, Science and Technology of Japan. KI was supported by the Japan Society for the Promotion of Science for Young Scientists. The use of synchrotron radiation for this work was approved by the Photon Factory Advisory Committee and KEK (High Energy Accelerator Research Organization), Tsukuba (proposal Nos. 2005G060 and 2006G171).

References

Ashikawa, Y., Fujimoto, Z., Noguchi, H., Habe, H., Omori, T., Yamane, H. & Nojiri, H. (2005). *Acta Cryst.* F**61**, 577–580.
Ashikawa, Y., Fujimoto, Z., Noguchi, H., Habe, H., Omori, T., Yamane, H. & Nojiri, H. (2006). In the press.
Batie, C. J., Ballou, D. P. & Correll, C. C. (1991). *Chemistry and Biochemistry of Flavoenzymes*, Vol. 3, edited by F. Muller, pp. 543–556. Boca Raton: CRC Press.
Bradford, M. M. (1976). *Anal. Biochem.* **72**, 248–254.
Bressler, D. C. & Fedorak, P. M. (2000). *Can. J. Microbiol.* **46**, 397–409.
Ferraro, D. J., Gakhar, L. & Ramaswamy, S. (2005). *Biochem. Biophys. Res. Commun.* **338**, 175–190.
Furukawa, K., Suenaga, H. & Goto, M. (2004). *J. Bacteriol.* **186**, 5189–5196.
Habe, H., Chung, J.-S., Lee, J.-H., Kasuga, K., Yoshida, T., Nojiri, H. & Omori, T. (2001). *Appl. Environ. Microbiol.* **67**, 3610–3617.
Habe, H. & Omori, T. (2003). *Biosci. Biotechnol. Biochem.* **67**, 225–243.
Inoue, K., Habe, H., Yamane, H. & Nojiri, H. (2006). *Appl. Environ. Microbiol.* **72**, 3321–3329.
Inoue, K., Habe, H., Yamane, H., Omori, T. & Nojiri, H. (2005). *FEMS Microbiol. Lett.* **245**, 145–153.
Inoue, K., Widada, J., Nakai, S., Endoh, T., Urata, M., Ashikawa, Y., Shintani, M., Saiki, Y., Yoshida, T., Habe, H., Omori, T. & Nojiri, H. (2004). *Biosci. Biotechnol. Biochem.* **68**, 1467–1480.
Matthews, B. W. (1968). *J. Mol. Biol.* **33**, 491–497.
Nam, J.-W., Noguchi, H., Fujimoto, Z., Mizuno, H., Ashikawa, Y., Abo, M., Fushinobu, S., Kobashi, K., Wakagi, T., Iwata, K., Yoshida, T., Habe, H., Yamane, H., Omori, T. & Nojiri, H. (2005). *Proteins*, **58**, 779–789.
Nam, J.-W., Nojiri, H., Noguchi, H., Uchimura, H., Yoshida, T., Habe, H., Yamane, H. & Omori, T. (2002). *Appl. Environ. Microbiol.* **68**, 5882–5890.
Nojiri, H., Ashikawa, Y., Noguchi, H., Nam, J.-W., Urata, M., Fujimoto, Z., Yoshida, T., Habe, H. & Omori, T. (2005). *J. Mol. Biol.* **351**, 355–370.
Nojiri, H., Nam, J.-W., Kosaka, M., Morii, K., Takemura, T., Furihata, K., Yamane, H. & Omori, T. (1999). *J. Bacteriol.* **181**, 3105–3113.
Nojiri, H. & Omori, T. (2002). *Biosci. Biotechnol. Biochem.* **66**, 2001–2016.
Otwinowski, Z. & Minor, W. (1997). *Methods Enzymol.* **276**, 307–326.
Sato, S., Nam, J.-W., Kasuga, K., Nojiri, H., Yamane, H. & Omori, T. (1997). *J. Bacteriol.* **179**, 4850–4858.
Takagi, T., Nojiri, H., Yoshida, T., Habe, H. & Omori, T. (2002). *Biotechnol. Lett.* **24**, 2099–2106.
Urata, M., Uchimura, H., Noguchi, H., Sakaguchi, T., Takemura, T., Eto, K., Habe, H., Omori, T., Yamane, H. & Nojiri, H. (2006). *Appl. Environ. Microbiol.* **72**, 3206–3216.
Wittich, R.-M. (1998). *Appl. Microbiol. Biotechnol.* **49**, 489–499.